ELSEVIER

Contents lists available at ScienceDirect

Applied Surface Science Advances

journal homepage: www.sciencedirect.com/journal/applied-surface-science-advances



Full Length Article



Antibacterial wool fabric with enhanced photostability, UV protection and hydrophilicity through surface acylation and TiO₂ nanocoating

Esfandiar Pakdel *0, Suju Fan 0, Jianming Chen, Xungai Wang *

Joint Research Centre for Fiber Innovations and Renewable Materials (JRC-FIRM), School of Fashion and Textiles, The Hong Kong Polytechnic University, Kowloon, Hong Kong

ARTICLE INFO

Keywords: Wool fabric Photostability UV protection Antibacterial textiles Superhydrophilicity

ABSTRACT

The development of functional textiles through applying nanocoatings has attracted significant attention in recent years. However, poor durability of nanocoatings highlights the necessity of modifying the surface chemistry of fibers to maximize the adherence of nanomaterials. In this study, the surface of wool fibers was modified through the acylation process with succinic anhydride and then post-treatment with anatase TiO2 colloid synthesized via the sol-gel method. Different aspects including the role of wool acylation on fibers chemistry, photostability, UV protection and antibacterial activity against Escherichia coli (E. coli) and Staphylococcus aureus (S. aureus) bacteria were discussed. Furthermore, wetting behavior, light and wash fastness, dyeability, and cytotoxicity of fabrics were investigated, and the role of each coating step was clarified. The findings confirmed that the modified fabric exhibited enhanced photostability under UVA radiation as tested using the photo-induced chemiluminescence (PICL) analysis. The functional fabric provided an excellent UPF level of 140, indicating 37 % improvement compared with pristine wool. The acylated fabric treated with TiO2 colloid was hydrophilic and showed a washing fastness up to five accelerated wash cycles. The existence of TiO2 led to a weaker color strength (K/S) on the dyed fabric, but did not photocatalytically affect the light fastness. The cytotoxicity test did not show any toxic effects on the examined cells viability. Moreover, comprehensive analyses using XPS, FTIR, SEM, and EDX mapping techniques were conducted to characterize the nano-treated fabrics. The outcomes of this research provide new insights on some less explored properties of functionalized textiles, paving the way for real-world applications.

1. Introduction

The surface modification of textiles using different types of nanoparticles such as ${\rm TiO_2}$, ZnO, Ag, Au, Pt, and MXenes to achieve novel functionalities has widely been explored [1]. For instance, antibacterial activity, thermoregulation, self-cleaning, electrical conductivity and superhydrophobicity are among the main features which have been explored [1–3]. Of various types of nanomaterials, titanium dioxide (${\rm TiO_2}$) is the most widely used semiconductor in developing functional textiles due to its low toxicity, cheap price, easy availability and feasible synthesis approach [4,5]. Through applying ${\rm TiO_2}$ nanoparticles on fibrous materials such as cotton, wool, polyester, silk, cashmere and viscose, novel features including photo-induced self-cleaning, UV protection and antibacterial activity have been achieved [1]. Due to its unique optical properties and wide band gap (3.2 eV for anatase ${\rm TiO_2}$), ${\rm TiO_2}$ shows photocatalytic activity only under ultraviolet radiation,

limiting its potential application in developing novel textile products [6, 7]. Therefore, great efforts have been made to enhance its sensitivity and photocatalytic response to visible light [8,9]. Modified forms of TiO₂ such as N-doped TiO2, noble metal-doped TiO2 nanostructures, dye-sensitized TiO2, TiO2/SiO2 nanocomposites and TiO2/semiconductors have been produced and used in developing textiles with enhanced functionalities [10,11]. The major focus of researchers in this field has mainly been on improving the light-induced functionalities of TiO₂-based nanomaterials; however, little attention has been paid to enhancing their durability on the functionalized textiles. Nanoparticles can be either applied to textiles surface in the form of coatings or incorporated into textile fibers as additives. In the latter case, the nanoparticles are embedded within the structure of fibers, reducing the likelihood of their detachment after multiple abrasions and washings, making this a safer option for developing functional products [3,12]. In contrast, nanoparticles which are used as coatings can be easily

E-mail addresses: esfandiar.pakdel@polyu.edu.hk (E. Pakdel), xungai.wang@polyu.edu.hk (X. Wang).

^{*} Corresponding authors.

detached from the textile substrates, weakening the performance of the finished products. The extent of this issue depends on the type of functionalized fibers and the used coating technique, and it is more pronounced in synthetic and protein-based fibers. In general, the detachment of nanoparticles from the coated textiles can lead to serious long-term consequences, such as contaminating water resources and endangering aquatic life. In addition, the detached nanoparticles may pose risk to human health through skin contact, inhalation, and ingestion, potentially causing health issues that are still largely unknown [1, 13]. Therefore, promoting the affinity and stability of nanoparticles onto textiles is of paramount importance and can contribute to developing products with minimized risks for consumers. The durability of nanocoatings on textiles relates to the surface characteristics of the coated surfaces and the interactions of nanocoatings with the fibers. It is necessary to obtain an optimal balance through modifying the existing coating techniques to not only increase the deposition rate of nanoparticles on textiles surface, but also to mitigate the potential risks to consumers.

Different techniques such as using cross-linking agents [5,14–16], coupling agents [17], enzymatic treatments [18], ultrasonication [19], plasma surface activation [20], and polymeric binders [21-23] have been reported to promote the durability of inorganic nanoparticles on coated textiles [24-26]. For instance, Zhu et al [27] immobilized Al₂O₃ nanoparticles on silk fibers via using tetra butyl titanate as a coupling agent, increasing the sunlight reflectivity to develop fabrics with passive radiative cooling functionality. Similarly, the application of various cross-linking agents such as citric acid, butane tetra carboxylic acid (BTCA) and β-cyclodextrin have been reported. Habib et al. [28] used citric acid to enhance the adhesion of Ag nanoparticles on cotton fabrics. The finished cotton samples showed strong antibacterial activity against E. coli and S. aureus bacteria. In other studies, carboxylic acids such as BTCA have been used as cross-linking agents to anchor TiO2 nanoparticles (P-25) onto wool fabrics to reduce photoyellowing of wool and to obtain a self-cleaning effect [29-31]. The wool fabrics were initially oxidized using potassium permanganate solution in an acidic solution, followed by treatment with nanoparticles in an ultrasonic bath containing cross-linking agents. It has also been reported that the surface modification of fibers via plasma pre-treatment can positively enhance the durability of coatings and nanoparticles on textiles [20,32]. Different gases such as oxygen, air, nitrogen, ammonia, and inert gases have been utilized to introduce new polar groups such as hydroxide, carbonyl, carboxyl, aldehyde, amino, etc. to fibers surface [32,33]. These functional groups act as new binding sites on fibers, enhancing the durability of applied coatings [33]. Another reported strategy is altering the morphology of fibers surface to affix the deposited nanoparticles. For instance, Zhao et al. [34] immobilized TiO₂ nanoparticles on the surface of polyacrylonitrile (PAN) fibers through inducing the swelling of fibers using dimethyl sulfoxide/ethanol solvent to embed TiO2 nanoparticles into the fibers surface. Among all reported methods, using polymer binders to develop durable coatings is probably the most effective way to affix nanoparticles onto textiles, but it can hamper the intrinsic properties of textiles such as hand feel, flexibility, air permeability and moisture absorption. Moreover, embedding nanoparticles in a polymer matrix may weaken their functionality for the intended applications. For example, Ag nanoparticles exhibit reduced antibacterial effectiveness for textiles when incorporated into a polydimethylsiloxane (PDMS) binder [22,35].

The acylation process has been reported as an effective approach in chemical modification of fibers particularly for protein fibers [36]. It is an established method to chemically modify the surface characteristics and functional groups of protein fibers for controlling water absorption and dye affinity [36,37]. For instance, Ranjbar-Mohammadi et al. [38] acylated the surface of wool fibers using succinic anhydride and phthalic anhydride followed by grafting with chitosan to develop antibacterial wool samples. Davarpanah et al. [39] used a similar approach to graft chitosan on the surface of silk fibers to achieve an antibacterial silk

fabric. The results revealed that the acylation process reduced the mechanical strength and dyeability of silk fibers [39]. Daoud et al. [40] modified wool fabric via the acylation process and then treated it with nano titanium dioxide to develop photocatalytic self-cleaning fabrics. However, no information was reported on other aspects of fabrics such as photostability, UV protection, dyeability and antibacterial activity.

Wool fibers intrinsically have several drawbacks such as severe photovellowing due to their sensitivity to UV radiation, poor surface wettability, and susceptibility to microbial attacks [41]. Therefore, innovative functional surface treatments are required to address the mentioned problems in wool fibers. Moreover, despite the progress in developing novel surface finishing techniques for textiles, tackling the poor durability of applied nanocoatings is still a major challenge. This study aims to chemically modify the surface of wool fibers via acylation with succinic anhydride to develop durable titania nanocoating on the fibers. The outcomes of this study will shed light on some under-explored areas by clarifying the synergistic effects of acylation and TiO₂ treatment on photostability, antibacterial activity, dyeability, and water absorption of treated wool fabrics. A comprehensive XPS analysis was conducted to clarify the effects of the finishing process on wool fibers surface chemistry. The photostability and UV protection of fabrics were examined based on the PICL analysis and measuring the UPF level of fabrics, respectively. The dyeability of fabrics with acid and reactive dyes was studied, followed by clarifying the effects of each treatment process on photoyellowing, photobleaching, and light fastness of fabrics. Antibacterial activity of fabrics was examined against E. coli and S. aureus bacteria, demonstrating the effectiveness of applied nanocoating in eradicating both types of bacteria. Moreover, other characterization techniques such as FTIR, TGA, SEM and EDX mapping were employed to provide a clearer picture on structural changes of modified fabrics and durability of nanocoatings.

2. Experimental

2.1. Materials and chemicals

Titanium tetra isopropoxide (TTIP) was used as the precursor of $\rm TiO_2$ nanoparticles and was purchased from the Sigma-Aldrich company. A 100 % wool fabric with an areal density of 225.2 g/m² was provided by Sunshine-Textile (China) company. Two types of dyes including Acid Green 50 (AG50) (CAS No 3087–16–9) and Reactive Red 2 (RR2) (CAS No 17,804–49–8) were used in dyeing the fabrics. Both succinic anhydride and N,N-Dimethylformamide (DMF) were purchased from the Sigma-Aldrich.

2.2. Synthesis of TiO2 colloid

 $\rm TiO_2$ colloid was synthesized with 5 % concentration through adding the predetermined amount of TTIP into the acidified water containing acetic acid [35]. The mixture was mixed and then 3.5 ml of HCl 37 % was added dropwise to the mixture followed by stirring for 2 h at 60 °C. The volume ratios of components in the synthesized colloid including water, HCl, glacial acetic acid, and TTIP were 88.6 %, 1.4 %, 5 %, 5 %, respectively. The synthesized nanoparticles were extracted through adding sodium carbonate powder to the acidic colloid, inducing the precipitation of $\rm TiO_2$ nanoparticles. The precipitated nanoparticles were collected, washed through centrifugation until neutral pH was obtained. The washed particles were dried in an oven at 80 °C for 8 h.

2.3. Acylation of wool fabric

Acylation (succinylation) of wool fabric was conducted in a DMF solvent containing 10 w/v % succinic anhydride at 60 $^{\circ}$ C for 2 h, followed by rinsing and drying. Prior to the succinylation process, wool fabric was scoured in a bath containing 2 g/L non-ionic detergent (Kieralon F-OL-B) at 50 $^{\circ}$ C for 30 min, followed by rinsing and drying.

2.4. Nano-TiO2 treatment of wool fabrics

The scoured and acylated wool fabrics were immersed into an ultrasonicated bath, followed by padding, drying and curing at 120 $^{\circ}$ C for 3 min. The coated fabrics were labelled as PW, AcylW, PW-TiO₂, and AcylW-TiO₂, representing the pristine wool, acylated wool, wool fabric treated with TiO₂ colloid, and acylated wool fabric treated with TiO₂ colloid, respectively.

2.5. Dyeing fabrics with acid and reactive dyes

Wool fabrics were dyed with AG50 and RR2 dyes, with the molecular structures shown in Fig 1, according to the procedure shown in Fig 2 using an oscillating dyeing machine (Hong Kong MX Dyeing Machine Co., LIMITED). The dyeing solutions were prepared based on adding 0.5 % o.w.f. dye into distilled water followed by adding 2 g/L sodium sulfate. Then, the pH of the dye solution was adjusted at about 3 by adding acetic acid. Liquid to good ratio was set at 1:50. After immersing wool fabrics in the dyeing solutions, temperature was raised to 95 °C with a heating rate of 1.5 °C/min, and it was kept constant for 60 min. The dyed fabrics were rinsed and dried in an oven at 50 °C. The changes of dye solutions concentration before and after the dyeing process were monitored based on UV–vis absorption spectra over 200–800 nm wavelength range.

2.6. Characterization techniques

Photostability of wool fabrics: Photostability of wool fabrics under UVA irradiation was tested based on the measured PICL peak intensity generated by wool fabrics after 30 s of exposure to UVA. The PICL analysis of fabrics was conducted using the Lumipol 3 chemiluminescence (CL) instrument (Polymer Institute, Slovak Academy of Sciences, Bratislava) equipped with an in-situ irradiation system with selectable wavelengths from a medium-pressure mercury arc (Lumatec SUV-DC, Lumatech GmbH, Germany). The test was conducted under controlled atmosphere (N2 and O2) at constant chamber temperature (40 °C) based on the testing protocol reported earlier [42]. Each fabric was cut circular in 8 mm diameter and exposed to 250–300 cm³/min N₂ gas flow in the instrument's chamber for 2 min for stabilization. This was followed by 30 s irradiation of samples under UVA light (320-400 nm). 60 s after stopping the irradiation, O2 gas was introduced to the test chamber, generating the PICL peak. The intensity of the PICL peak and then its decaying trend was recorded for 500 s.

UV-protection factor (UPF) of fabrics: UPF level of fabrics along with UVA and UVB transmittance rates through the fabrics were measured using a spectrophotometer (UPF and UV Penetration/Projection Measurement System, Model: YG902, China) according to the AS/NZS4399 standard. Eight different spots of fabrics were tested, and the average values were reported.

Antibacterial activity test: The antibacterial activity of fabrics was

assessed against gram-negative *E. coli* and gram-positive *S. aureus* according to the AATCC 100–2004 test method [8]. First, bacteria suspensions with the concentration of 1×10^7 colony forming units (CFU)/ml were prepared by adding microorganisms into tryptic soy broth. Each fabric was sterilized under UV irradiation for 45 min prior to testing. Each fabric was put in a sterile gamma container, and 1 mL of bacteria inoculum was added followed by incubation at 37 °C for 24 h. Next, 100 mL of saline was added to each container followed by vigorous shaking. 1 mL of the prepared solution was cultured in Petri dishes containing tryptic soy agar medium followed by incubation at 37 °C. After 24 h incubation period, the growth rate of bacteria colonies in each agar plate was observed and their photographs were recorded.

Cytotoxicity test: Cell biocompatibility of the samples was evaluated using l-929 cells. A density of 3000 cells per well was seeded in a 96-well plate containing 100 μL of complete Dulbecco's Modified Eagles Medium (DMEM) supplemented with Fetal bovine serum 10 % FBS and 1 % PS. After culturing for 24 h at 37 °C in a 5 % CO2 incubator, the culture media were replaced. In the experimental group, the media were substituted with DMEM incubated with the textile samples (10 g/L) for 24 h, while the control group received only complete DMEM. After 24 h incubation, 10 μL of CCK-8 was added to each well and incubated for 2 h at 37 °C. The absorbance of the experimental (Aexp), control (Ac), and blank (Ab) groups at a wavelength of 450 nm was measured using a microplate reader (Varioskan LUX). Four measurements were carried out for each sample, and the average values were reported. Cell viability was calculated using the Eq. (1).

$$Cell viability(\%) = (A_{exp} - A_b)/(A_c - A_b)$$
 (1)

Wettability and Moisture Management Test (MMT): The wettability of fabrics was tested based on measuring the water contact angle (WCA) using KSVCAM101 testing instrument. The MMT test was conducted using a moisture management tester (M290, SDL Atlas) through measuring the absorption rates of artificial sweat droplets on fabrics. The average values of at least three measurements for each sample were reported.

SEM images and EDX mappings were recorded using the Field Emission Scanning Electron Microscope (Tescan MIRA). TEM image of TiO2 nanoparticles was taken using JEOL TEM-2100F microscope (Japan). Fourier transform infrared spectroscopy (FTIR) tests were conducted using the Varian 1000 instrument equipped with an Attenuated total reflectance (ATR) attachment. The UV–vis spectra of TiO2 colloid and dye solutions were measured using a Varian-carry-300 spectrophotometer. X-ray diffractometer (XRD) pattern of the prepared TiO2 powder was obtained using X'Pert PRO MRD XL (PANalytical) instrument with a Cu K α radiation over 20 range of 20–80° operating at 40 kV and 30 mA. The surface chemistry of coated fabrics was characterized using the X-ray photoelectron spectroscopy (XPS) (Thermo Fisher Scientific Nexsa) technique, and atomic ratios of detected elements on the outer surface of coatings were calculated.

Color specifications of fabrics: The color indices were measured

Fig. 1. The molecular structures of a) AG50 and b) RR2 dyes.

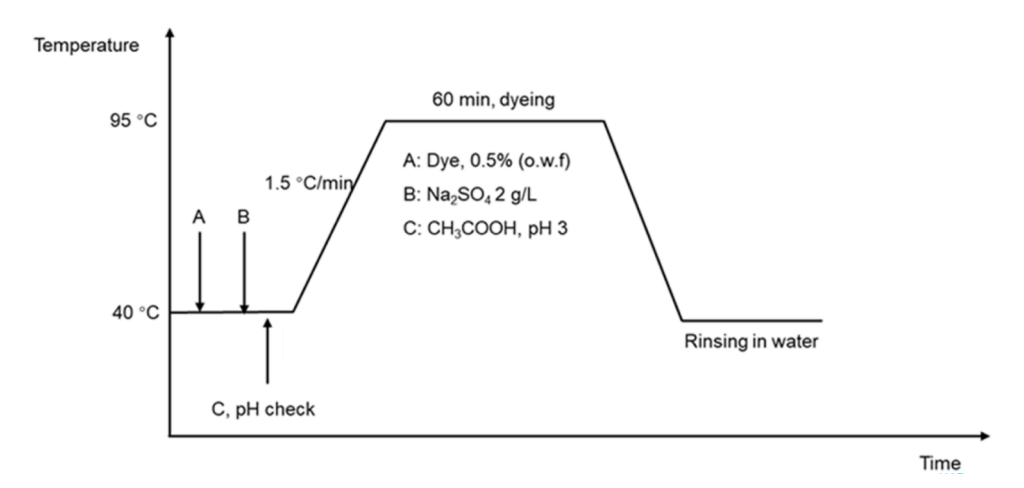


Fig. 2. Dyeing procedure of wool fabrics with AG50 and RR2 dyes.

using a Datacolor (Spectraflash, SF 600-Plus, USA) spectrophotometer. The fabrics were tested under D65 illumination source in a CIE L* a*b* system, and their color variation ($\triangle E$) was calculated according to the Eq. (2).

$$\Delta E = \sqrt{(\Delta L^*)^2 + (\Delta a^*)^2 + (\Delta b^*)^2}$$
 (2)

where L* represented the lightness of the fabric (lighter if positive; darker if negative), and a* and b* showed the red-green (redder if positive; greener if negative) and yellow-blue colors (yellower if positive; bluer if negative) of the fabrics, respectively. The color strength of

fabrics (K/S) was calculated based on the reflectance (R) values of fabrics using the same Datacolor spectrophotometer. (Eq. (3))

$$K/S = (1-R)^2/2R$$
 (3)

where K and S were the absorption and scattering coefficients of fabrics, respectively.

Light and washing fastness testing: The light fastness of dyed fabrics was tested based on the variation of color of fabrics after 40 h exposure to Xenon light. The photoyellowing and photobleaching of undyed fabrics were calculated based on measuring the variations of their

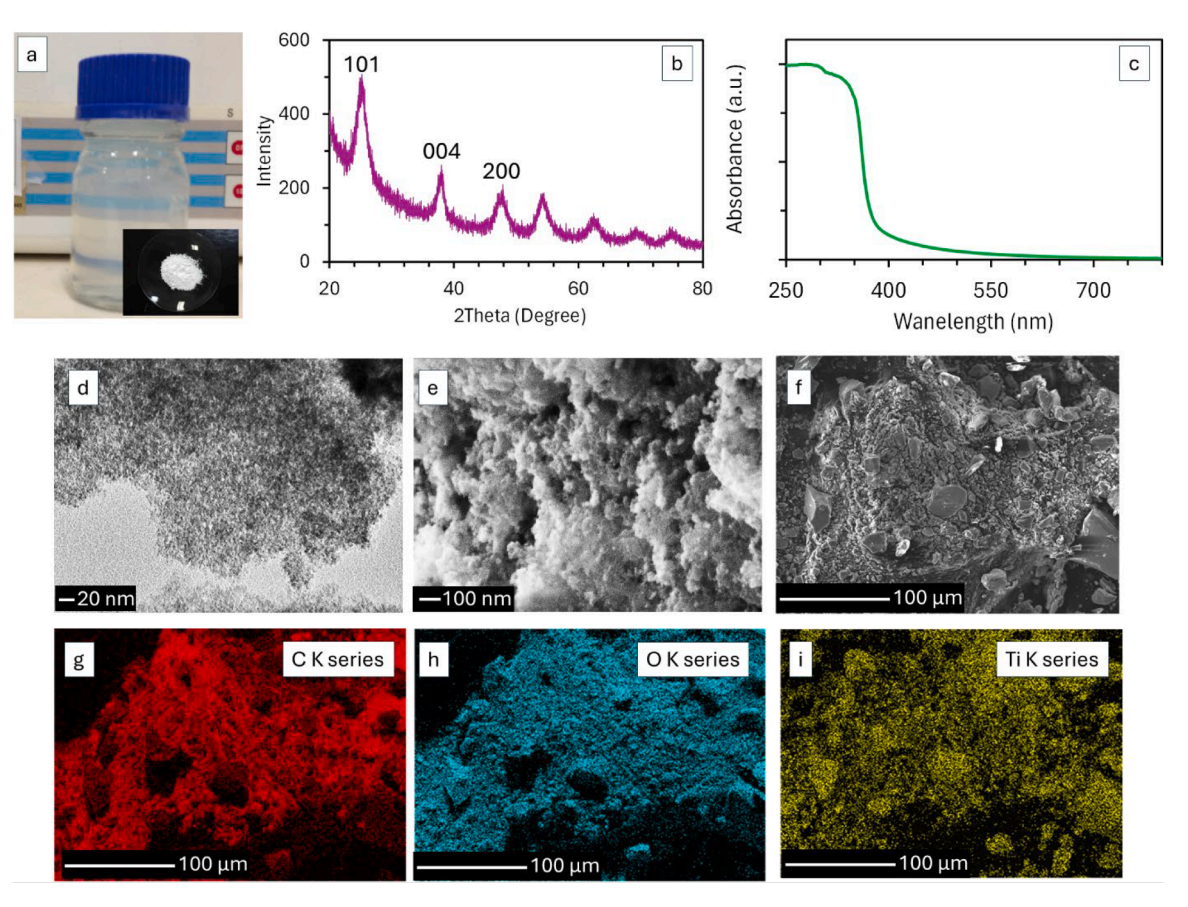


Fig. 3. a) TiO₂ colloid synthesized through the sol-gel method (The inset image shows the extracted TiO₂ powder from the colloid via the precipitation method), b) XRD pattern of the synthesized TiO₂ nanoparticles, c) UV–Vis spectrum of the synthesized colloid, d) TEM and e) SEM images of the extracted TiO₂ nanoparticles, f-i) SEM and the corresponding EDX mappings of TiO₂ nanoparticles.

yellowness and whiteness indices. The washing process of AcylW-TiO $_2$ fabric was done using the Launder-Ometer machine based on the AATCC 61–2010 standard test method. The fabric (10 cm \times 5 cm) was washed five times, and each wash cycle was performed in a canister containing 150 mL water with 4 g/L detergent and 10 steel balls at 40 $^{\circ}$ C for 30 min.

3. Results and discussion

3.1. Characterization of the synthesized TiO2 colloid

The TiO₂ colloid was synthesized through the low-temperature solgel method and a semi-transparent bluish TiO₂ colloid was obtained (Fig 3a). XRD pattern of the extracted TiO₂ powder demonstrated the anatase crystalline structure of the synthesized nanoparticles, showing characteristic peaks at $2\theta=25.2^\circ,~37.92^\circ,~47.62^\circ,~$ and 54.25° which represented the planes of 101, 004, 200, and 211 of TiO₂ nanocrystalline structure, respectively (Fig 3b) [43,44]. The UV–vis absorption of TiO₂ sharply increased at $\lambda <$ 400 nm, demonstrating the intrinsic UV absorption behavior of TiO₂ nanoparticles (Fig 3c). TEM and SEM images showed TiO₂ nanoparticles aggregation with individual particles size around <20 nm (Fig 3d and e). For SEM imaging of TiO₂ powder, no conductive surface coating was applied on TiO₂ nanoparticles, revealing the porous structure of the synthesized nanoparticles (Fig 3e). The EDX mapping displayed the existence and distribution of Ti, O, and C elements in the structure of the extracted powder as shown in Fig 3f-i.

3.2. Characterization of wool fabrics

3.2.1. Scanning electron microscopy (SEMs)

The effect of acylation and treatment with titania colloid on surface morphology of fibers was analyzed using SEM images (Fig 4). Fig 4a shows the typical morphology of a pristine wool fiber, characterized with flattened overlapping surface cuticle scales arranged from root to tip direction of fiber. This outer protective layer has a sulfur-rich composition acting as a protective sheath around inner cuticle cells, determining several features such as wettability of fibers, dyeability, surface tension and friction [45]. After acylation, the scales were still clear, but some smoothened scales edges and foreign matters deposited on AcylW fibers were noticeable. Moreover, on the PW-TiO₂ fibers, a thin layer of TiO₂ was formed which was significantly thicker on the AcylW-TiO₂ sample. The applied TiO₂ nanoparticles covered the edges

of the scales, indicating the deposition of a greater loading of nanoparticles on the acylated fibers. This can be attributed to the presence of more surface anchoring sites on the acylated fibers, facilitating the attachment of nanoparticles. EDX mapping of AcylW-TiO $_2$ detected the existence of C, O, N, S, and Ti elements in the treated fiber. It was observed that the TiO $_2$ nanoparticles distributed evenly all over the fiber surface, smoothing out the natural unevenness of the surface. In general, it can be said that this coating technique, i.e., acylation of fabric and then treatment with TiO $_2$ colloid, produced a more uniform distribution of nanoparticles on fibers compared with the previously reported coating method based on the surface oxidation of wool and then ultrasonic-assisted coating of TiO $_2$ (P-25) nanoparticles [46,47].

3.2.2. FTIR and TGA of wool fabrics

The effect of acylation on chemical configuration of wool fabrics was assessed using FTIR analysis (Fig 5a). The characteristic peaks of wool appeared at 1510 cm⁻¹ and 1640 cm⁻¹ which were assigned to Amid II (Bending vibrations of N—H bonds) and Amid I (Stretching vibrations of the C = O bond) in the fiber structure, respectively [48]. The small peak appeared at 1230 cm⁻¹ was related to Amid III, which is associated with the C-N stretching and N-H in-plane bending. After acylation, two new peaks were detected at 1730 cm⁻¹ and 1150 cm⁻¹, resulting from the existence of free carbonyl groups, formed by anhydride ring opening, and the formation of C-O-C bonds with wool surface, respectively [38, 40]. TGA thermographs (Fig 5b) of wool fabrics showed that the acylation process weakened the thermal stability of wool, as the main weight loss onset temperature shifted from 263 °C for PW to 212 °C for AcylW. This could be related to the effect of acylation process on the dissociation of disulfide bonds in the structure of wool fibers. Also, it has been reported that the acylation process can accelerate the molecular movement within the wool polymer chain and destabilize the structure of the α -helix crystalline structure within wool fibers [49]. The total weight loss of PW and AcylW fabrics were calculated as $-89.9\ \%$ and $-96.2\ \%,$ respectively, clearly showing the effect of acylation on reducing the thermal stability of wool.

3.2.3. XPS analysis

To better explore the surface chemistry changes of wool fibers after each treatment, XPS analysis was conducted (Fig 6) [50]. The XPS surveys showed the presence of four key elements of C, O, S, and N in the structure of untreated and modified wool samples, although with

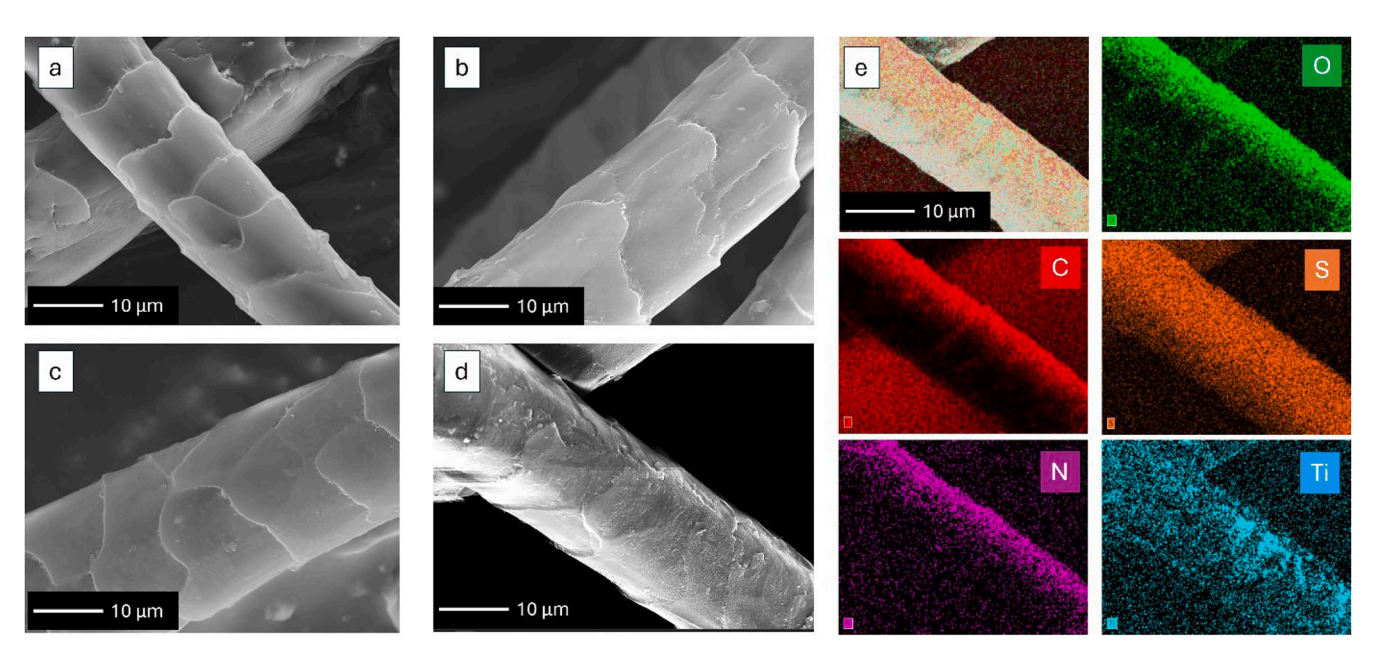


Fig. 4. SEM images of a) PW, b) AcylW, c) PW-TiO2, and d) AcylW-TiO2 fibers; e) EDX mapping of AcylW-TiO2 fiber.

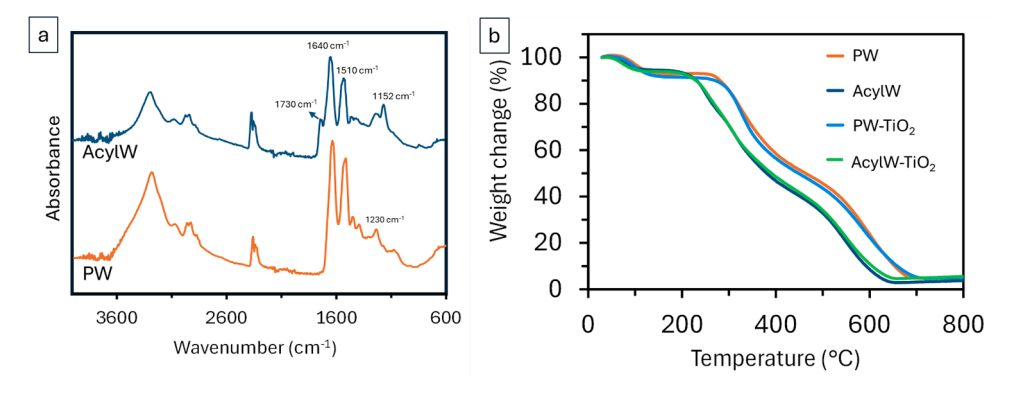


Fig. 5. a) FTIR spectra and b) TGA analysis of wool fabrics.

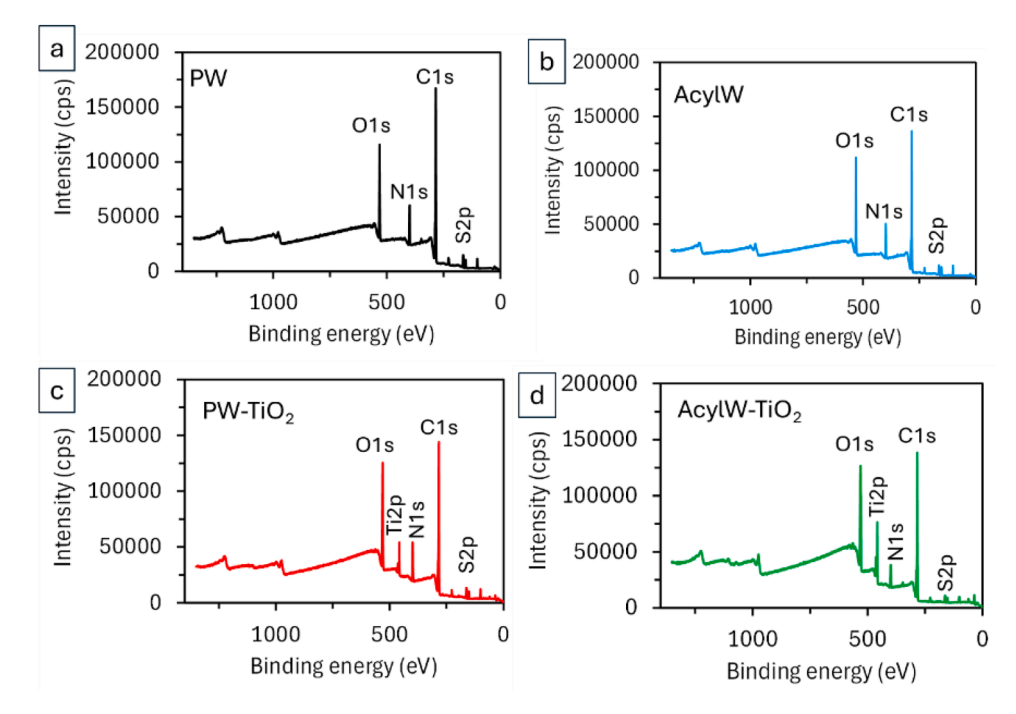


Fig. 6. XPS survey of a) PW, b) AcylW, c) PW-TiO2, and AcylW-TiO2 fabrics.

varying intensities. For untreated wool sample, i.e. PW, the peaks of O1s, C1s, N1s, and S2p were found at binding energies of 531 eV, 284.5 eV, 400 eV, and 164 eV, respectively. The origin of the detected O1s peak

could be attributed to the existence of Amide and some hydrophilic chemical groups in the structure of fibers [48]. The sharp peak of C1s was from the fatty-acid monolayer which exists on the epicuticle layer of

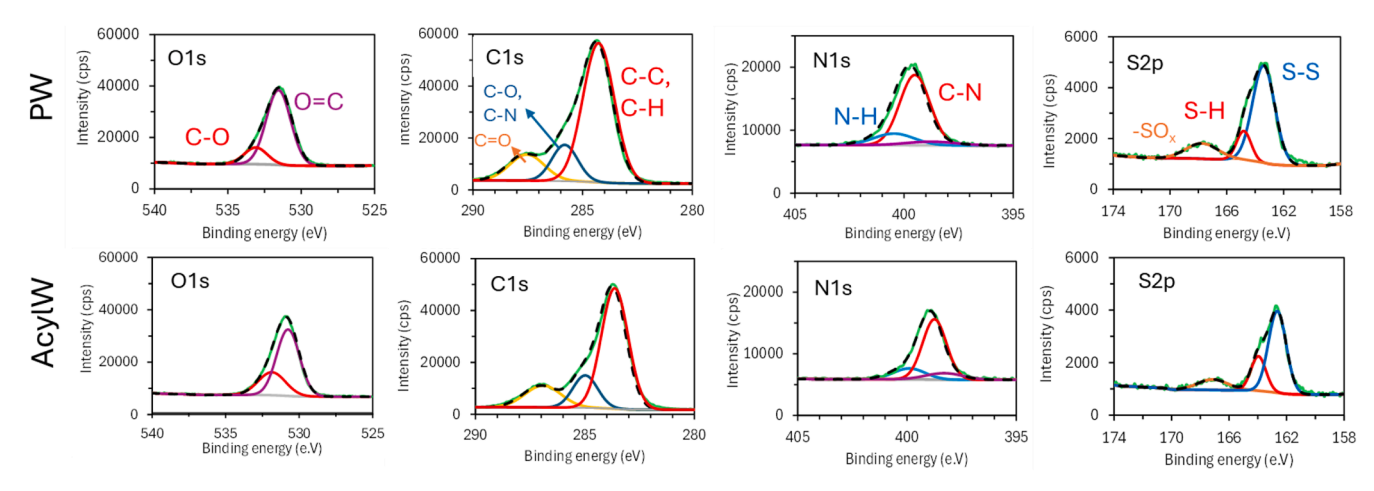


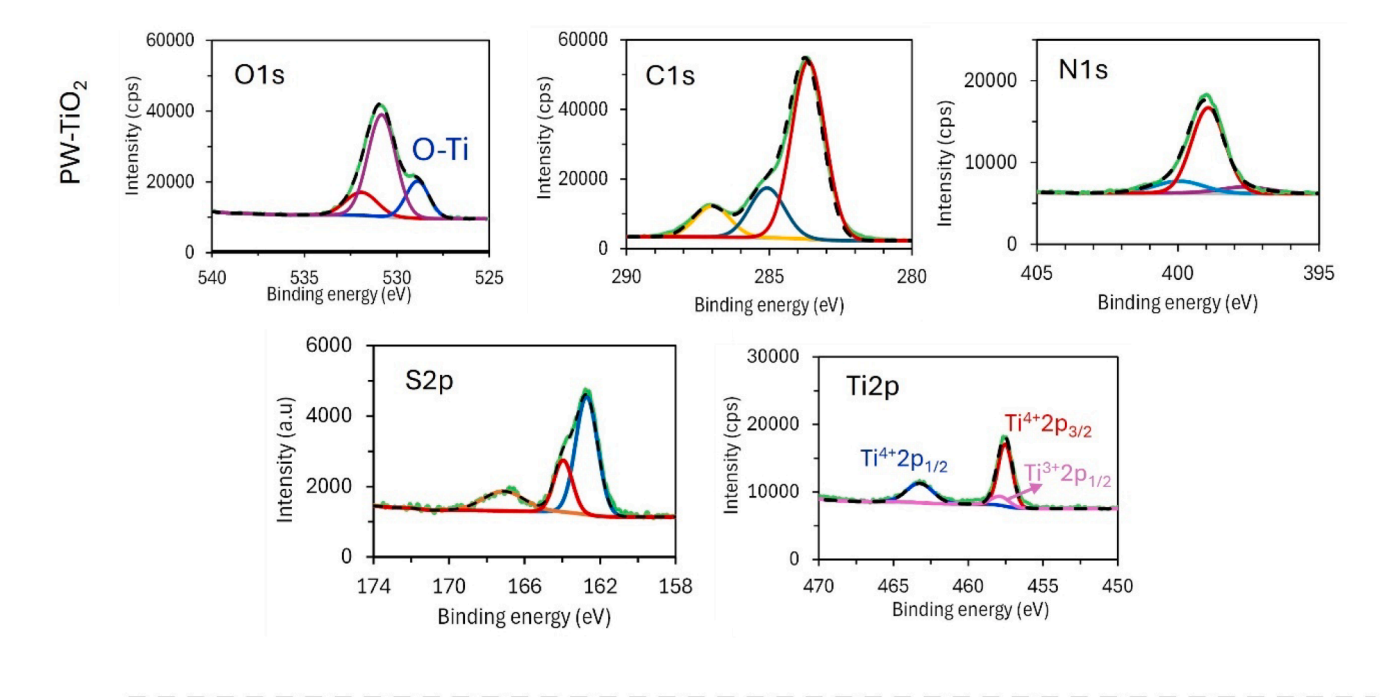
Fig. 7. High resolution XPS analysis of PW and AcylW fabrics.

outer surface of wool fibers and contains a high concentration of carbon [51]. The intensity of the C1s peak declined after the acylation process which can be related to the removal of upper layer of fatty acid from the fibers surface [51]. The N1s and S2p peaks mainly stemmed from amino acid cystine within the structure of cuticle layer [52]. After treating the fabrics with TiO $_2$ colloid, the Ti 2P peak appeared at 457.6 eV, indicating the deposition of TiO $_2$ nanoparticles (Figs 6c and d). A stronger Ti2p peak was detected from the pretreated sample, implying the deposition of a greater amount of TiO $_2$ nanoparticles on the fabric.

High resolution XPS spectra of PW and AcylW fibers (Fig 7) and their deconvoluted peaks showed that the O1s peak mainly composed of two smaller peaks located at 531.4 eV and 533 eV, representing the existence of O = C and O–C bonds on the outer layer of wool fiber surface. The peak of C1s of PW was deconvoluted into three smaller peaks located at

284.3 eV, 285.8 eV, and 287.5 eV, which were ascribed to the existence of C–C/C–H, C–N/C–O, and –C $\stackrel{-}{=}$ O bonds on the wool fiber surface. After acylation, these peaks moved to 283.6 eV, 285.1 eV, and 286.9 eV positions, respectively, indicating the removal of surface lipid layer [53, 54]. The main deconvoluted S2p peaks were found at 163.4 eV, 164.7 eV, and 167.8 eV which were ascribed to the presence of disulfide (–S–S $^{-}$) bonds, S–H functional group, and sulfur oxide compounds (–SO $_{\rm X}$), respectively [54–56]. After acylation, the peaks shifted to lower binding energy and the overall intensity of S2p peaks decreased. The reduction of the S–S bonds and stronger S–H peak signal confirmed that some disulfide bonds were damaged after carrying out the acylation process [55].

As shown in Fig 8, after the treatment of fabrics with TiO_2 colloid, new peaks related to Ti2p appeared at binding energies of 457.6 eV and



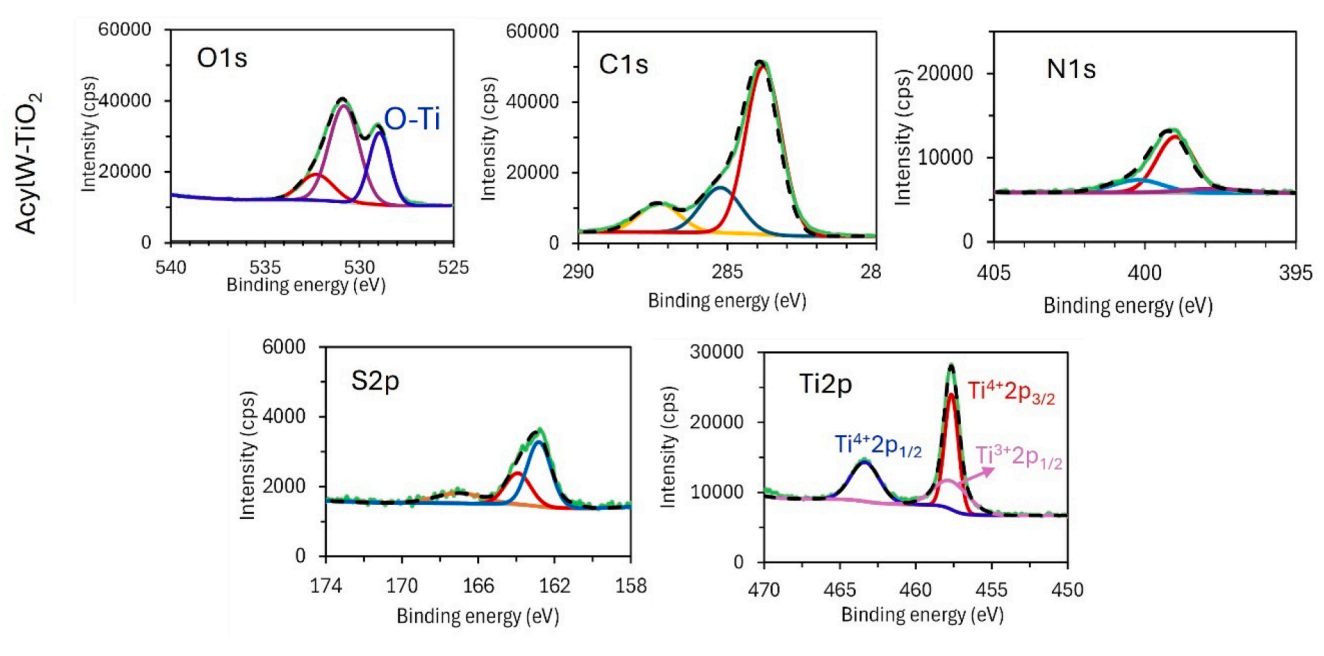


Fig. 8. High resolution XPS spectra of pristine and acylated wool fabrics after treatment with TiO2 colloid.

463.2 eV, representing $Ti2p_{3/2}$ and $Ti2p_{1/2}$, respectively [35,57]. Moreover, the deconvoluted O1s peak at 529 eV was due to the existence of O-Ti bond and the existence of lattice oxygen bound to Ti⁴⁺[58]. It was noted that the Ti2p peaks were sharper on the AcylW-TiO₂ sample due to the deposition of a higher quantity of TiO2 on the surface of fiber. A weak peak at 457.8 eV was found which was related to the existence of Ti³⁺ defect in the structure of the synthesized TiO₂ nanoparticles. This may influence on the photocatalytic activity of TiO₂ nanoparticles under visible light as reported earlier [35]. The observation of stronger Ti2p peaks on AcylW-TiO2 fabric compared with PW-TiO2 sample was in good agreement with the calculated atomic concentration of Ti on fabrics as listed in Table 1. Also, the N1s and S2p peaks became weaker compared with other tested fabrics which can be due to the formation of a thicker coating layer on fabrics, and less accessibility of these elements for the XPS detector, considering that the XPS technique can only test top outer surface layer of fibers.

Three main functional groups of wool keratin which are found in the side chains are carboxyl group (–COOH), amino group (–NH $_2$) and hydroxyl group (–OH) [59,60]. By altering the configuration of cysteine in the cuticle layer, it is expected to have newly formed –SH functional groups on the wool surface [60]. Through reacting succinic anhydride with wool's functional groups, new carboxyl groups can be introduced to wool fiber surface [61]. Therefore, based on the conducted FTIR and XPS analyses, the mechanism of wool surface modification through the discussed acylation pretreatment and then titania nanocoating can be proposed as shown in Fig 9.

3.2.4. Photostability and UV protection

The effect of the applied treatments on wool fabrics photostability was evaluated based on the PICL analysis (Fig 10a and b). In this testing approach, wool samples were exposed to the irradiation of UV light for 30 s under N2 atmosphere, which resulted in the generation of polymer free radicals in wool and triggering its photodegradation reactions. These excited species generated chemiluminescence peak after reaction with oxygen gas, which was introduced to the testing chamber 60 s after stopping the irradiation period. Therefore, the population of these excited polymer species in wool samples was referred to as an indication of the effect of UV light on wool samples [62,63]. The deposition of TiO₂ nanoparticles, which are intrinsically considered as strong UV absorbers, on the surface of wool could potentially reduce the absorption of incident UV light by wool, thereby reducing the photodegradation pace and enhancing the photostability of wool samples [42]. Both natural and synthetic polymer fibers emit luminescence upon exposure to visible and UV light, a phenomenon which is known as photoinduced chemiluminescence [64]. In fact, the incident light can be absorbed by light-absorbing photo-initiators present in polymer fibers which may be chromophores or oxidation products, and cause the generation of polymer free radicals and charge separation [63]. Two main intermediates for the generation of PICL are macroperoxy radicals (PO'2) and polymer hydroperoxides (POOH·), which can be generated by the reaction of polymer radicals with oxygen [65,66]. The application of TiO₂ nanoparticles to the surface of wool to form a UV-protective barrier on fibers reduces the production rate of polymer radicals and therefore reduces the PICL peak intensity [42]. As shown in Fig 10a and b, through carrying out the acylation modification on wool fabric and then subsequent modification with TiO2, the PICL peak intensity reduced by 83.5

 $\begin{tabular}{ll} \textbf{Table 1} \\ \textbf{The atomic ratio (\%) of detected elements on pristine, acylated and coated wool fabrics.} \\ \end{tabular}$

	O1s	C1s	N1s	S2p	Ti2p	O/C	Ti/C
Raw wool	16.3	72.12	8.75	2.84	-	0.23	-
AcylW	18.5	70.58	8.43	2.49	-	0.26	-
Wool-TiO ₂	20.41	66.26	8.18	2.54	2.62	0.31	0.04
AcylW-TiO ₂	23.98	63.57	5.80	1.69	4.96	0.38	0.08

% and 45 %, compared with PW and PW-TiO₂ samples, respectively. This could be related to the decreased concentration of light-absorbing chromophores in the structure of AcylW, and also the deposition of a greater amount of TiO_2 nanoparticles on fibers, providing a better protective shield against incident UV.

The UV protection level of fabrics was compared based on the measured UPF levels (Fig 10c). Based on the results, the UPF levels of PW-TiO₂ and AcylW-TiO₂ samples were 133.8 and 138.9, respectively, which were 31 % and 37 %, higher than that of PW fabric. Evaluating the UV transmittance (T %) rates through the fabrics over UVA (315-400 nm) and UVB (280-315 nm) regions, showed that the UVA transmittance rate of fabrics changed more noticeably. The AcylW-TiO₂ sample had the lowest T % over the UVA range compared with other tested samples. The measured T % for AcylW-TiO2 fabric over UVA wavelength range was 2.71 %, while for PW and PW-TiO2, it was 4.21 % and 2.8 %, respectively. The acylation pre-treatment had a negligible effect on these values, and it can be said that the deposition rate of TiO_2 nanoparticles on fabrics played the key role in enhancing the UV protection of fabric. The changing trends of UPF values corroborated the PICL results, showing an enhanced photostability and UV protection after acylation and TiO2 treatments.

The UV protection mechanism of ${\rm TiO_2}$ nanoparticles is related to the absorption of incoming photon energy by valence band electrons of ${\rm TiO_2}$ and generating pairs of ${\rm e}^-/h^+$ in a femtosecond time [67]. This process excites electrons from the valence band of ${\rm TiO_2}$ to the conduction band, producing pairs of negative conduction band electrons (e) and valence band holes (h^+) [67]. The photogenerated products can rapidly recombine, releasing their energy in the form of heat or light. Therefore, based on this mechanism, they can minimize the UV damage to the coated fibers. However, if the photogenerated species escape from the recombination process, they initiate photocatalytic redox reactions, producing photocatalytic functionality [67].

3.2.5. Wettability and moisture management property of fabrics

Testing the wettability of fabrics (Fig 11) demonstrated that the PW, PW-TiO2 and AcylW samples were hydrophobic with WCA values of 95.6°, 111.7°, and 131.2°, respectively. It is known that the untreated wool fiber is naturally hydrophobic, due to the existence of a thin fatty acids layer on its epicuticle, having been covalently bound to the protein matrix [68]. This hydrophobic property of wool causes issues in different characteristics of wool such as sweat absorption, dyeability and uptaking finishing agents [69,70]. The hydrophobicity of the AcylW was because of the presence of hydrophobic acyl chains on the wool fibers surface, acting as a protective layer against water molecules [36]. However, after treatment of the acylated wool with the titania colloid, the AcylW-TiO2 fabric became superhydrophilic, and the measured WCA reduced to 0°. Based on the MMT analysis, it was found that the absorption rates of artificial sweat droplets were 268.3 \pm 28.0 %/s and 28.5 ± 2.0 %/s on AcylW-TiO₂ and PW fabrics, respectively, confirming the rapid liquid absorption on the coated fabric.

3.2.6. Dyeability of wool fabrics

The prepared wool fabrics were dyed with AG50 and RR2 dyes and the obtained color change (ΔE) and color strength (K/S) of fabrics were measured. Table 2 indicates the details of color specifications of each wool fabric before and after the dyeing process. As a general trend, it was observed that TiO₂ treatment affected the color of wool fabrics by increasing their lightness (L*). Also, the presence of TiO₂ nanoparticles on fabrics increased the ΔE value in the dyed fabrics, which could be related to the unevenness in the fabrics color, and non-uniform light reflection from the fabrics surface. Based on the appearance of dyed wool fabrics (Fig 12a), it can be said that the acylation process resulted in a darker color shade, while TiO₂ treatment reduced the color depth of dyed fabrics. These observations were also corroborated by the measured K/S values of fabrics. Based on the measured K/S values, the color strength of AcylW sample was higher than that of PW (Fig 12b).

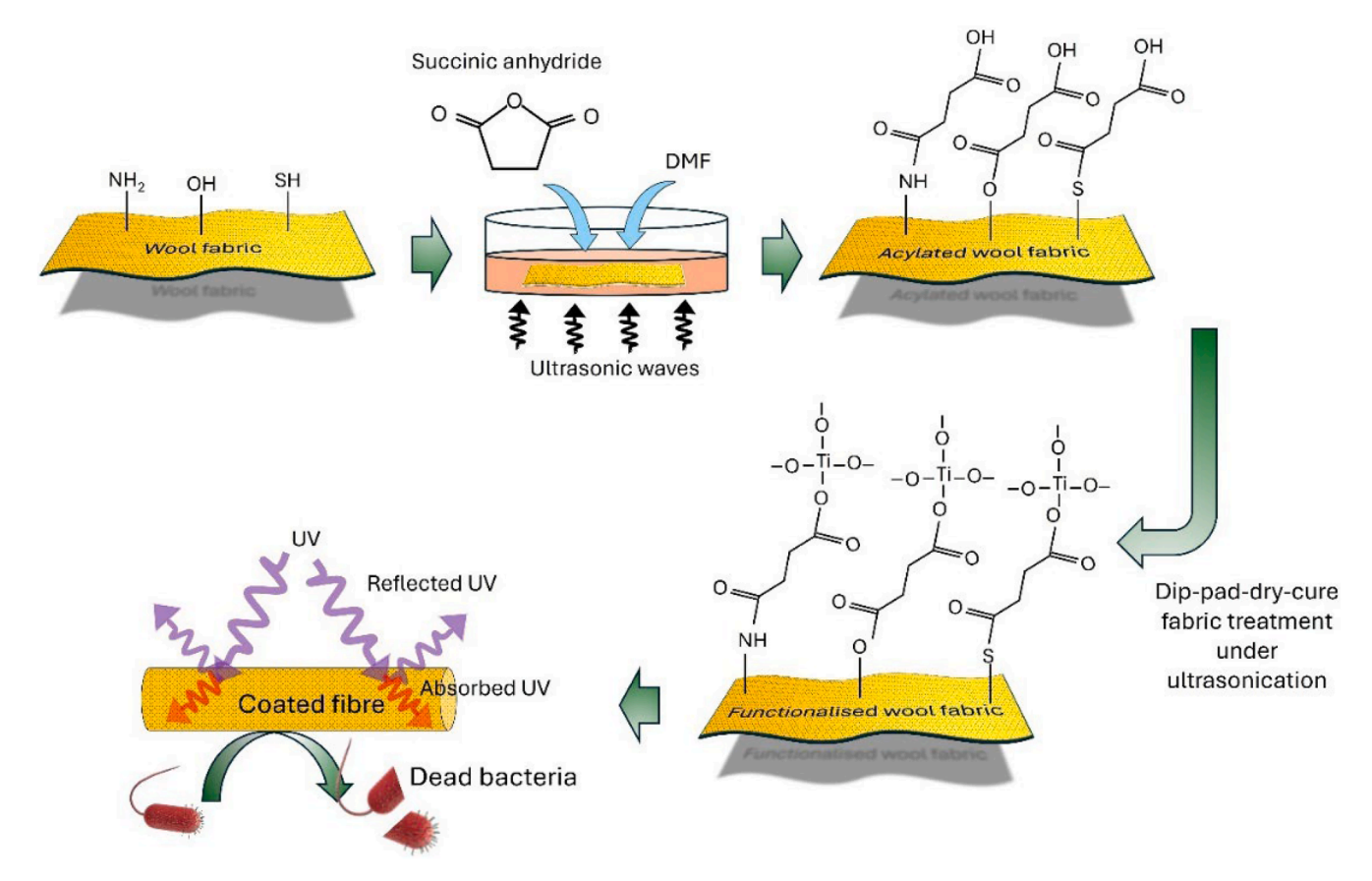


Fig. 9. The proposed mechanism of wool surface acylation and attachment of TiO2 nanoparticles to the wool fiber surface.

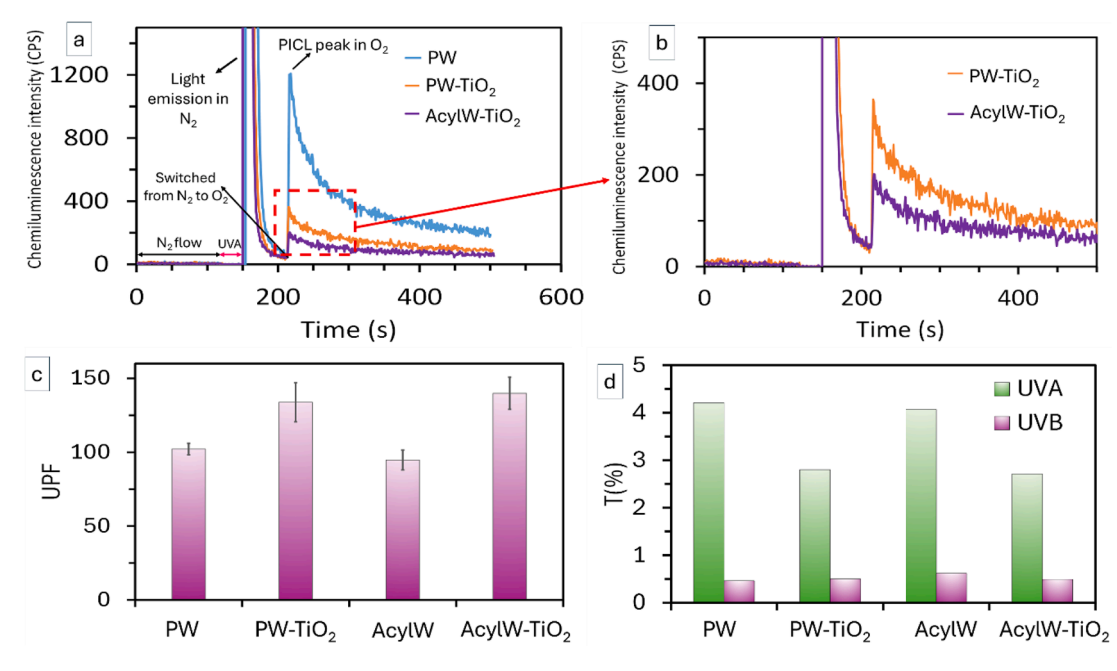


Fig. 10. a) PICL spectra of wool fabrics in O₂ after exposure to UVA radiation, b) comparison of the effect of acylation process on the PICL peak intensity, c) UPF values of fabrics and d) UV transmittance rates through fabrics over UVA and UVB regions.

This was related to the structural changes in AcylW, which allowed more dye molecules to penetrate the inner parts of wool, creating stronger color depths. The presence of TiO₂ reduced the K/S value of the dyed fabrics, likely due to its natural white color and high refractive index, which altered the response of the coated fabrics to incident light during

the color measurement test.

The photostability of undyed and dyed wool fabrics was further analyzed by monitoring the variations of fabrics whiteness (ΔW) and yellowness (ΔY) after 40 h exposure to Xenon light (Fig 12c). It was found that the PW underwent a severe photobleaching process, and the

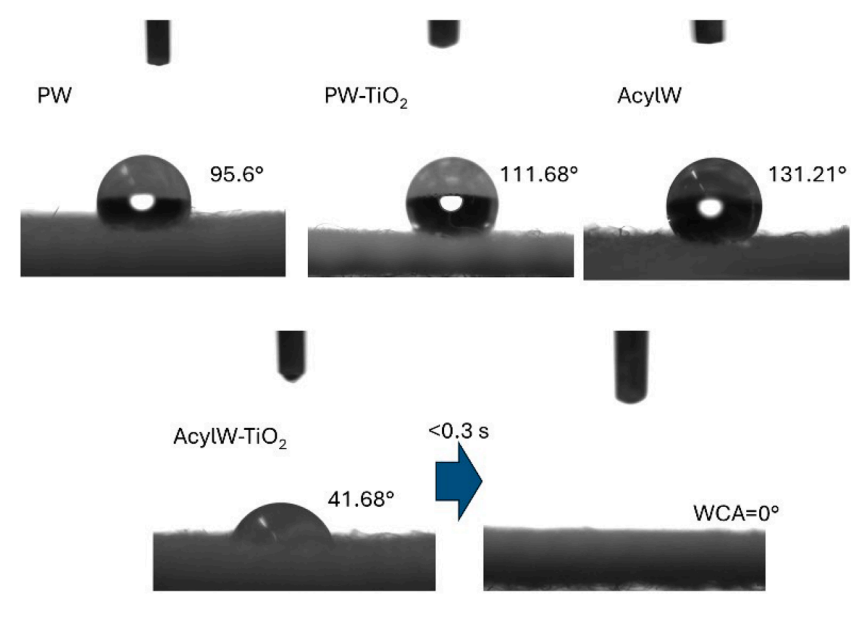


Fig. 11. WCA of pristine, acylated and coated wool fabrics.

Table 2Color indices of wool fabrics before and after dyeing with AG50 and RR2 dyes.

				, ,	•
Samples	L*	a*	b*	ΔE (Compared with PW)	ΔE (Compared with the corresponding undyed fabric)
PW	80.2	-1.2	8.5	_	_
PW-TiO ₂	82.6	-1.5	9.2	2.5	_
AcylW	80.1	-1.1	8.2	0.3	_
AcylWTiO ₂	81.0	-0.7	11.5	3.1	_
PW-AG50	49.1	-29.1	-7.0	44.6	44.6
PW-TiO ₂ - AG50	49.8	-29.6	-4.8	43.7	45.4
AcylW-AG50	48.2	-30.0	-5.8	45.3	45.2
AcylWTiO ₂ - AG50	47.9	-30.7	-4.7	45.7	47.5
PW-RR2	47.0	52.5	-0.9	63.8	63.8
PW-TiO ₂ - RR2	48.7	52.2	-1.0	62.7	64.4
AcylW-RR2	46.8	53.9	2.3	64.7	65.0
AcylWTiO ₂ - RR2	46.7	54.3	1.7	65.2	65.0

color of the fabric became whiter, and the measured ΔW and ΔY values were 11.2 and -3.5, respectively. After applying TiO_2 coating to PW, the photobleaching process in the fabric slowed down and the measured ΔW reduced to 5.3. After 40 h of irradiation, the yellowness of AcylW increased noticeably (ΔY =2.6), causing a severe yellow color in the fabric. But after coating the AcylW with TiO_2 nanoparticles, both photoyellowing and photobleaching trends in the AcylW- TiO_2 fabric slowed down dramatically, and the calculated changes in yellowness and whiteness of fabrics were ΔY =-1.8 and ΔW =2.5, respectively, implying the enhanced photostability of fabrics.

The color change of dyed fabrics after 40 h irradiation was also examined (Fig 12d). In overall, the observed ΔE variation in fabrics dyed with AG50 dye was greater than the samples dyed with RR2, which can be related to different chemical structures of dyes and their different levels of light fastness. TiO_2 is known for its superior photocatalytic activity under UV irradiation, and the utilized Xenon light spectrum contained a small portion of UVA, simulating daylight. However, it was realized that the photocatalytic feature of TiO_2 did not significantly accelerate the color fading of the fabrics after 40 h of irradiation. This can be due to having a very small portion of UV in the simulated sunlight and also the deposition of a very low amount of TiO_2 nanoparticles on

fibers.

3.2.6. Antibacterial activity and cytotoxicity assessments

Antibacterial activity of nano-treated fabrics against E. coli and S. aureus bacteria was tested (Fig 13a). Both AcylW-TiO2 and PW-TiO2 samples provided a strong bactericidal effect against both types of bacteria, and the acylation process did not have any deteriorating effect on the fabric's antibacterial performance. Antibacterial activity can result from the photo-induced activity of TiO2 nanoparticles. Although the antibacterial test was conducted without any direct UV irradiation on samples, it would be plausible to say that the antibacterial activity of TiO₂ nanoparticles might have activated because of the surrounding light causing the observed antibacterial effect. TiO2 can generate photoinduced pairs of electrons (e_{VB}) and positive holes (h_{CB}^+) after absorbing the incoming photons energy. These species react with surrounding oxygen and water molecules, producing superoxide anions (O₂⁻) and hydroxyl radicals (OH·) [71,72]. These products are reactive and can readily interact with surrounding organic compounds such as bacteria cell walls, causing the leakage of macromolecular compounds such as proteins, minerals, and generic materials, leading to the death of bacteria [25,73]. Additionally, some researchers have reported the mechanisms of antimicrobial activity of TiO2 nanoparticles in dark and in the absence of any irradiation source. For instance, Vargas et al. [74] reported that the dark antimicrobial activity of TiO2 nanoparticles can be related to the presence of surface oxygen vacancies and Ti³⁺ below the conduction band of TiO2. The interaction of oxygen and water molecules with oxygen vacancies can lead to the formation of superoxide radical groups, which can contribute to the enhancement of the antibacterial effect. It has also been reported that the oxygen vacancies of TiO₂ nanoparticles can react with the dissolved oxygen, and produce radicals such as 'OH, 'O2, and HO2, giving rise to an antibacterial activity [75, 76]. Our XPS results confirmed the presence of surface defects of Ti³⁺in the synthesized TiO₂ nanoparticles. Therefore, the role of surface oxygen vacancies is mentioned as one of the contributing mechanisms in obtaining effective bactericidal activity on wool fabrics.

Testing the cytotoxicity of coated fabrics showed that the deposition of TiO_2 nanoparticles did not result in any noticeable changes in l-929 cell's viability (Fig 13b). The results showed that the cells viability rates did not change noticeably in the presence of AcylW-TiO₂ sample compared with PW and PW-TiO₂. It should be highlighted that there are some disagreements in the literature regarding the potential toxic effects of nanomaterials and particularly TiO_2 nanoparticles. In general, it

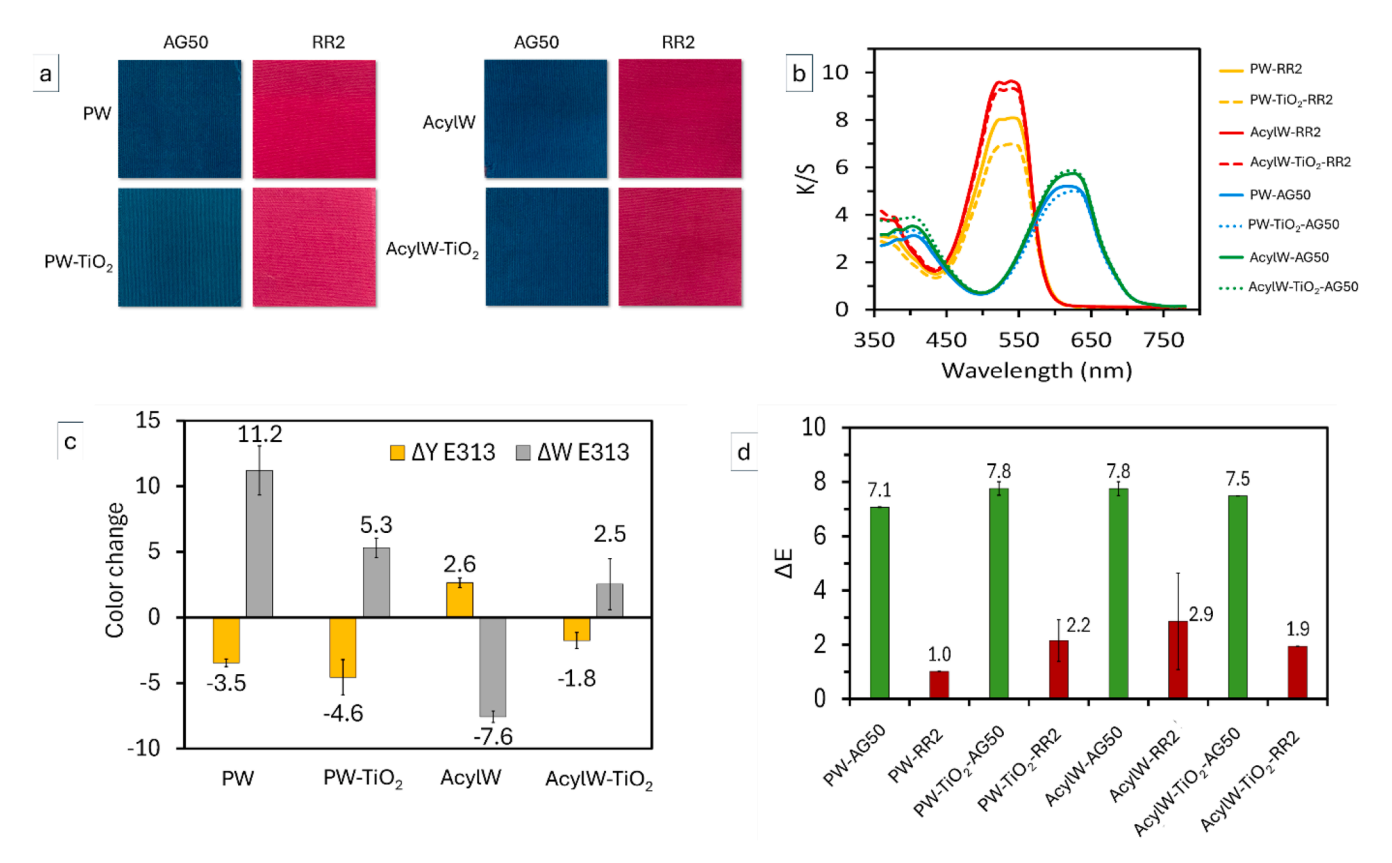


Fig. 12. a) The appearance of dyed wool fabrics, b) K/S spectra of dyed fabrics over visible wavelengths, c) photobleaching and photoyellowing of pristine and modified fabrics after 40 h exposure to Xenon light, d) photostability of dyed fabrics after 40 h exposure to Xenon light.

seems that there is no consensus on the standard test method which should be utilized for assessing the effects of nanoparticles, especially if they are applied to textile substrates. Based on the literature, the toxicity of nanoparticles varies based on their shape, size, crystallinity, surface area, synthesis method and even the application methods on textiles [77, 78]. In general, the employed techniques of applying nanoparticles to textiles, the immobilization methods, pre-treatment of textiles, and the type and chemistry of fibrous substrates, all are contributing factors which can influence on the rate of detachment of nanoparticles from the fibers surface and their overall toxicity [1,79].

The washing fastness of AcylW-TiO $_2$ fabric was also tested (Fig 13c). The sample was washed in an accelerated condition in the presence of detergent. Analyzing the surface morphology of the washed fabric using SEM imaging and EDX mapping confirmed the existence of TiO $_2$ nanoparticles on the surface of the washed fabric, confirming the durability of applied coatings on acylated wool fabric. To better evaluate the washing fastness of the applied nanocoating, a piece of pristine wool fabric was sewn to the AcylW-TiO $_2$ fabric during the washing process. This allowed us to check if there is any detachment and possible migration of nanoparticles to the adjacent wool fabric. Based on the SEM image (Fig 13d), no evidence of transferring TiO $_2$ nanoparticles to the adjunct fiber was observed, confirming the high durability of applied coatings on the tested wool fabric.

4. Conclusion

In this study, the effects of acylation process with succinic anhydride on various properties of wool fabric including the adsorption of ${\rm TiO_2}$ nanoparticles, photostability, antibacterial activity, wettability, and dyeability were investigated. A comprehensive analysis was conducted to understand the potential changes in the chemistry and morphology of wool fabric at each stage of surface treatment, including acylation and dip-coating with ${\rm TiO_2}$ colloid. Based on the XPS results, it was found that

the acylation pre-treatment increased the oxygen content on fibers outer surface while moderately reduced the amounts of nitrogen, carbon and sulfur elements. It was also demonstrated that a higher loading of TiO2 nanoparticles was deposited on the acylated fabric. The PICL analysis confirmed that the acylation process and TiO2 treatment synergistically contributed to the higher photostability of wool fabric. In addition, these treatments reduced photobleaching and photoyellowing rates in wool fabric after 40 h exposure to the simulated sunlight. The AcylW-TiO₂ fabric provided the UPF level of 140 which is an excellent UV protection level for textiles. It aslo exhibited an effective antibacterial activity against both E. coli and S. aureus bacteria with 100 % bacterial eradication efficiency. The results showed that the acylation process increased the colour strength (K/S) of fabrics dyed with AG50 and RR2 dyes, while TiO2 reduced it. The photocatalytic activity of TiO2 nanoparticles did not cause any color fading in wool fabrics even after 40 h of continuous irradiation. The coated acylated wool fabric showed a good washing fastness, and no significant cytotoxicity effect was observed. The outcomes of this study provided a comprehensive analysis on surface modification of wool fibers, through acylation and nano TiO2 treatment to impart more durable functionalities to textile products.

Declaration of generative AI and AI-assisted technologies in the writing process

No AI tools were used in preparation and writing of this manuscript.

CRediT authorship contribution statement

Esfandiar Pakdel: Writing – original draft, Methodology, Investigation, Formal analysis, Data curation, Conceptualization. **Suju Fan:** Investigation. **Jianming Chen:** Investigation. **Xungai Wang:** Writing – review & editing, Supervision.

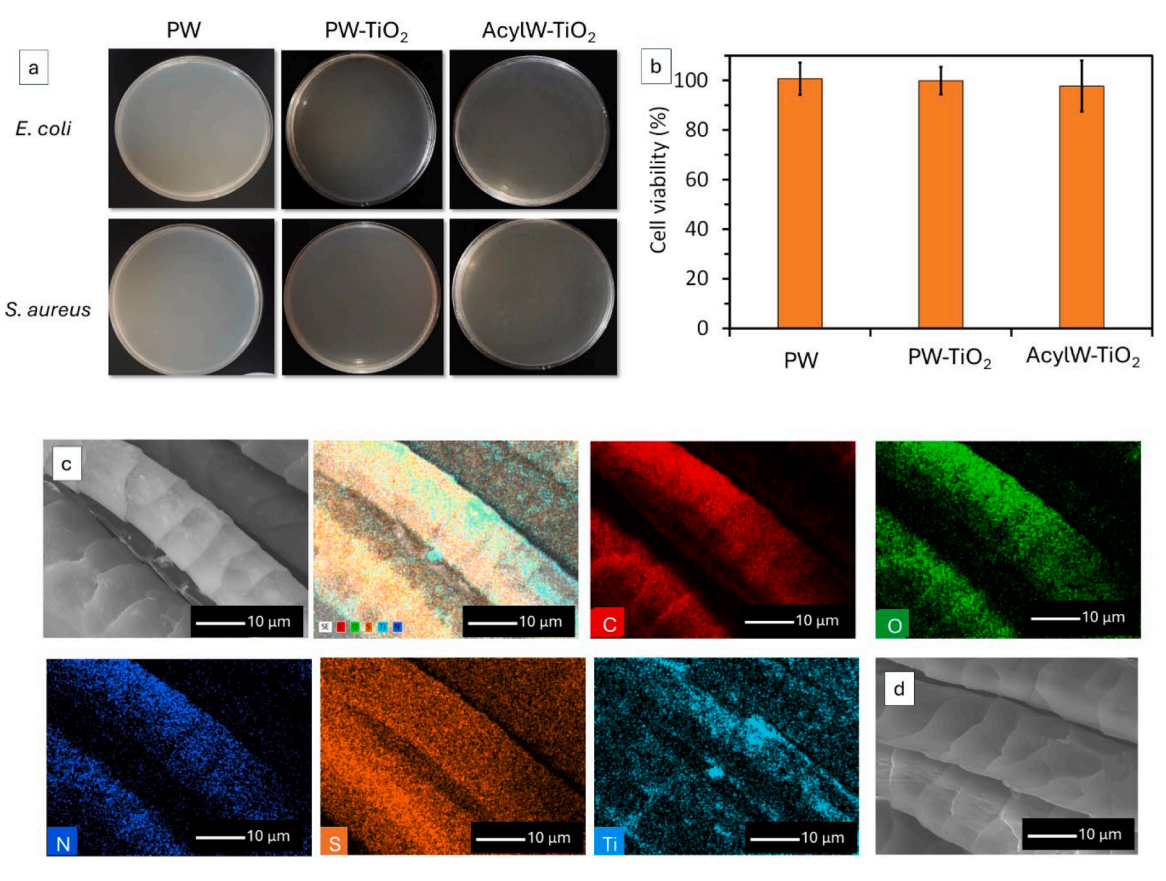


Fig. 13. a) Antibacterial activity of fabrics against *E. coli* and *S. aureus* bacteria, and b) cytotoxicity test of wool fabrics; c) washing fastness of AcylW-TiO₂ sample based on SEM image and EDX mapping analyses; d) the control wool fabric used during the washing process.

Declaration of competing interest

The authors declare that they have no known competing financial interests or personal relationships that could have appeared to influence the work reported in this paper.

Acknowledgement

This work was financially supported by the Hong Kong Polytechnic University.

Data availability

The data cannot be shared at this time as the data forms part of an ongoing study.

References

- E. Pakdel, J. Wang, S. Kashi, L. Sun, X. Wang, Advances in photocatalytic self-cleaning, superhydrophobic and electromagnetic interference shielding textile treatments, Adv. Colloid Interface Sci 277 (2020) 102116, https://doi.org/10.1016/i.cis.2020.102116.
- [2] A.K. Yetisen, H. Qu, A. Manbachi, H. Butt, M.R. Dokmeci, J.P. Hinestroza, M. Skorobogatiy, A. Khademhosseini, S.H. Yun, Nanotechnology in textiles, ACS Nano 10 (2016) 3042–3068, https://doi.org/10.1021/acsnano.5b08176.
- [3] E. Pakdel, X. Wang, Thermoregulating textiles and fibrous materials for passive radiative cooling functionality, Mater. Des 231 (2023) 112006, https://doi.org/ 10.1016/j.matdes.2023.112006.
- [4] M. Radetić, Functionalization of textile materials with TiO₂ nanoparticles, J. Photochem, Photobiol, C 16 (2013) 62–76, https://doi.org/10.1016/j. iphotochemrey 2013 04 002
- [5] C.K. Kundu, L. Song, Y. Hu, Chitosan-metal oxide nanoparticle hybrids in developing bi-functional polyamide 66 textiles with enhanced flame retardancy and wettability, Appl, Surf, Sci, Adv 7 (2022) 100202, https://doi.org/10.1016/j. apsadv.2021.100202.

- [6] E. Pakdel, W.A. Daoud, X. Wang, Assimilating the photo-induced functions of TiO₂-based compounds in textiles: emphasis on the sol-gel process, Text, Res, J 85 (2014) 1404–1428, https://doi.org/10.1177/0040517514551462.
- [7] Z. Li, Z. Li, C. Zuo, X. Fang, Application of nanostructured TiO₂ in UV photodetectors: a review, Adv, Mater 34 (2022) 2109083, https://doi.org/10.1002/adma.202109083.
- [8] E. Pakdel, W.A. Daoud, X. Wang, Effect of the photoreduction process on the self-cleaning and antibacterial activity of Au-doped TiO₂ colloids on cotton fabric, ACS Appl. Mater. Interfaces 16 (2024) 25221–25235, https://doi.org/10.1021/acsami.4c01238.
- [9] G.T. Kenda, C.G. Fotsop, D.R.T. Tchuifon, P.A.N. Kouteu, T.F. Fanle, S.G. Anagho, Building TiO₂-doped magnetic biochars from Citrus sinensis peels as low-cost materials for improved dye degradation using a mathematical approach, Appl, Surf, Sci, Adv 19 (2024) 100554, https://doi.org/10.1016/j.apsadv.2023.100554.
- [10] M.M. Rashid, B. Simončič, B. Tomšić, Recent advances in TiO₂-functionalized textile surfaces, Surf. Interfaces 22 (2021) 100890, https://doi.org/10.1016/j. surfin.2020.100890.
- [11] V. Etacheri, C. Di Valentin, J. Schneider, D. Bahnemann, S.C. Pillai, Visible-light activation of TiO₂ photocatalysts: advances in theory and experiments, J. Photochem, Photobiol, C: Photochem, Rev 25 (2015) 1–29, https://doi.org/ 10.1016/j.jphotochemrev.2015.08.003.
- [12] S. Zeng, S. Pian, M. Su, Z. Wang, M. Wu, X. Liu, M. Chen, Y. Xiang, J. Wu, M. Zhang, Q. Cen, Y. Tang, X. Zhou, Z. Huang, R. Wang, A. Tunuhe, X. Sun, Z. Xia, M. Tian, M. Chen, X. Ma, L. Yang, J. Zhou, H. Zhou, Q. Yang, X. Li, Y. Ma, G. Tao, Hierarchical-morphology metafabric for scalable passive daytime radiative cooling, Science 373 (2021) 692–696, https://doi.org/10.1126/science.abi5484.
- [13] S. kazemi, A. Hosseingholian, S.D. Gohari, F. Feirahi, F. Moammeri, G. Mesbahian, Z.S. Moghaddam, Q. Ren, Recent advances in green synthesized nanoparticles: from production to application, Mater, Today Sustain 24 (2023) 100500, https://doi.org/10.1016/j.mtsust.2023.100500.
- [14] L. Wu, X. Bao, Z. Li, Y. Yu, Y. Liu, B. Xu, M. Zhou, Q. Wang, P. Wang, Rapid photothermal antibacterial and antifungal textiles through dynamic disulfide bond-assisted in-situ deposition of SeNPs, Chem, Eng, J 479 (2024) 147772, https://doi.org/10.1016/j.cei.2023.147772
- [15] R.R. Gadkari, A. Gupta, U. Teke, A. Awadhiya, M. Shahadat, W. Ali, A. Das, R. Alagirusamy, A sustainable way for surface functionalisation of PET nonwoven with novel chitosan-cinnamaldehyde cross-linked nanoparticles, J. Ind, Eng, Chem 99 (2021) 214–223, https://doi.org/10.1016/j.jiec.2021.04.031.
- [16] J. An, F. Zou, J. Zhang, B. Tang, J. Wang, Enhanced properties of silk fabric through immobilization of gold and titanium dioxide nanoparticles, Colloids Surf,

- A: Physicochem, Eng, Asp 634 (2022) 128018, https://doi.org/10.1016/j.colsurfa.2021.128018.
- [17] S. Bhattacharjee, R. Joshi, M. Yasir, A. Adhikari, A.A. Chughtai, D. Heslop, R. Bull, M. Willcox, C.R. Macintyre, Graphene- and nanoparticle-embedded antimicrobial and biocompatible cotton/silk fabrics for protective clothing, ACS Appl, Bio Mater 4 (2021) 6175–6185, https://doi.org/10.1021/acsabm.1c00508.
- [18] L. Paza, W.C. Vicente, M. Miotto, M.A. Provenzi, D.A. Netzel, L.N. Carli, P. B. Brondani, Surface treatment of polyamide 6 through enzymatic hydrolysis and covalent incorporation of chitosan nanoparticles, Biomacromolecules 26 (2025) 981–991, https://doi.org/10.1021/acs.biomac.4c01281.
- [19] T. Harifi, M. Montazer, A review on textile sonoprocessing: a special focus on sonosynthesis of nanomaterials on textile substrates, Ultrason, Sonochem 23 (2015) 1–10, https://doi.org/10.1016/j.ultsonch.2014.08.022.
- [20] M. Radetić, D. Marković, A review on the role of plasma technology in the nanofinishing of textile materials with metal and metal oxide nanoparticles, Plasma Process. Polym 19 (2022) 2100197, https://doi.org/10.1002/ppap.202100197.
- [21] E. Pakdel, J. Sharp, S. Kashi, W. Bai, M.P. Gashti, X. Wang, Antibacterial superhydrophobic cotton fabric with photothermal, self-cleaning, and ultraviolet protection functionalities, ACS Appl. Mater. Interfaces 15 (2023) 34031–34043, https://doi.org/10.1021/acsami.3c04598.
- [22] E. Pakdel, S. Kashi, J. Sharp, X. Wang, Superhydrophobic, antibacterial, and EMI shielding properties of Ag/PDMS-coated cotton fabrics, Cellulose 31 (2024) 3921–3946, https://doi.org/10.1007/s10570-024-05819-7.
- [23] E. Pakdel, W. Xie, J. Wang, S. Kashi, J. Sharp, Q. Zhang, R.J. Varley, L. Sun, X. Wang, Superhydrophobic natural melanin-coated cotton with excellent UV protection and personal thermal management functionality, Chem, Eng, J 433 (2022) 133688, https://doi.org/10.1016/j.cej.2021.133688.
- [24] A. Patti, Green advances in wet finishing methods and nanoparticles for daily textiles, Macromol, Rapid Commun 46 (2025) 2400636, https://doi.org/10.1002/ marc.202400636.
- [25] E. Pakdel, J. Fang, L. Sun, X. Wang, Nanocoatings for smart textiles, in: N.D. Yilmaz (Ed.), Smart Textiles: Wearable Nanotechnology, Wiley, Hoboken, 2018, pp. 247–300, https://doi.org/10.1002/9781119460367.ch8.
- [26] M.P. Gashti, E. Pakdel, F. Alimohammadi, Nanotechnology-based coating techniques for smart textiles, in: J. Hu (Ed.), Active Coatings for Smart Textiles, Woodhead Publishing, Duxford, 2016, pp. 243–268, https://doi.org/10.1016/ B978-0-08-100263-6.00011-3.
- [27] B. Zhu, W. Li, Q. Zhang, D. Li, X. Liu, Y. Wang, N. Xu, Z. Wu, J. Li, X. Li, P. B. Catrysse, W. Xu, S. Fan, J. Zhu, Subambient daytime radiative cooling textile based on nanoprocessed silk, Nat, Nanotechnol 16 (2021) 1342–1348, https://doi.org/10.1038/s41565-021-00987-0.
- [28] S. Habib, F. Kishwar, Z.A. Raza, Citrate-mediated impregnation of silver nanoparticles for durable antibacterial cellulosic fabric, Pigment, Resin Technol 53 (2024) 240–248, https://doi.org/10.1108/PRT-06-2022-0077.
- [29] M. Montazer, E. Pakdel, M. Moghadam, Nano titanium dioxide on wool keratin as UV absorber stabilized by butane tetra carboxylic acid (BTCA): a statistical prospect, Fibers Polym 11 (2010) 967–975, https://doi.org/10.1007/s12221-010-0067 y.
- [30] M. Montazer, E. Pakdel, Self-cleaning and color reduction in wool fabric by nano titanium dioxide, J. Text, Inst 102 (2011) 343–352, https://doi.org/10.1080/ 00405001003771242.
- [31] M. Montazer, E. Pakdel, A. Behzadnia, Novel feature of nano-titanium dioxide on textiles: antifelting and antibacterial wool, J. Appl, Polym, Sci 121 (2011) 3407–3413, https://doi.org/10.1002/app.33858.
- [32] R. Thompson, D. Austin, C. Wang, A. Neville, L. Lin, Low-frequency plasma activation of nylon 6, Appl, Surf, Sci 544 (2021) 148929, https://doi.org/10.1016/ j.apsusc.2021.148929.
- [33] M. Naebe, A.N.M.A. Haque, A. Haji, Plasma-assisted antimicrobial finishing of textiles: a review, Engineering 12 (2022) 145–163, https://doi.org/10.1016/j. eng 2021 01 011
- [34] J. Zhao, J. Wang, L. Fan, E. Pakdel, S. Huang, X. Wang, Immobilization of titanium dioxide on PAN Fiber as a recyclable photocatalyst via Co-dispersion solvent dip coating, Tex, Res, J 87 (2017) 570–581, https://doi.org/10.1177/ 0040517516632479
- [35] E. Pakdel, W.A. Daoud, S. Kashi, M. Parvinzadeh Gashti, X. Wang, Superhydrophilic self-cleaning cotton fabric with enhanced antibacterial and UV protection properties, Cellulose 32 (2025) 1937–1958, https://doi.org/10.1007/ s10570-024-06346-1.
- [36] T. Arai, G. Freddi, R. Innocenti, D.L. Kaplan, M. Tsukada, Acylation of silk and wool with acid anhydrides and preparation of water-repellent fibers, J. Appl, Polym, Sci 82 (2001) 2832–2841, https://doi.org/10.1002/app.2137.
- [37] N.N. Shah, N. Soni, R.S. Singhal, Modification of proteins and polysaccharides using dodecenyl succinic anhydride: synthesis, properties and applications—A review, Int, J. Biol, Macromol 107 (2018) 2224–2233, https://doi.org/10.1016/j. ijbiomac.2017.10.099.
- [38] M. Ranjbar-Mohammadi, M. Arami, H. Bahrami, F. Mazaheri, N.M. Mahmoodi, Grafting of chitosan as a biopolymer onto wool fabric using anhydride bridge and its antibacterial property, Colloids Surf. B Biointerfaces 76 (2010) 397–403, https://doi.org/10.1016/j.colsurfb.2009.11.014.
- [39] S. Davarpanah, N.M. Mahmoodi, M. Arami, H. Bahrami, F. Mazaheri, Environmentally friendly surface modification of silk fiber: chitosan grafting and dyeing, Appl, Surf, Sci 255 (2009) 4171–4176, https://doi.org/10.1016/j. apsusc.2008.11.001.
- [40] W.A. Daoud, S.K. Leung, W.S. Tung, J.H. Xin, K. Cheuk, K. Qi, Self-cleaning Keratins, Chem, Mater 20 (2008) 1242–1244, https://doi.org/10.1021/ cm702661k.

- [41] F. Khosravi, M. Montazer, Chapter 16 microbial attack and prevention methods: microbial attack on wool fiber, causes, and remedies, in: S. Jose, S. Thomas, G. Basu (Eds.), The Wool Handbook, Woodhead Publishing, 2024, pp. 357–379, https://doi.org/10.1016/B978-0-323-99598-6.00004-9.
- [42] E. Pakdel, W.A. Daoud, L. Sun, X. Wang, Reprint of: photostability of wool fabrics coated with pure and modified TiO₂ colloids, J. Colloid Interface Sci 447 (2015) 191–201, https://doi.org/10.1016/j.jcis.2015.01.076.
- [43] T.Z. Liza, M.M.H. Tusher, F. Anwar, M.F. Monika, K.F. Amin, F.N.U. Asrafuzzaman, Effect of Ag-doping on morphology, structure, band gap and photocatalytic activity of bio-mediated TiO₂ nanoparticles, Results Mater 22 (2024) 100559, https://doi. org/10.1016/j.rinma.2024.100559.
- [44] E. Pakdel, W.A. Daoud, S. Seyedin, J. Wang, J.M. Razal, L. Sun, X. Wang, Tunable photocatalytic selectivity of TiO₂/SiO₂ nanocomposites: effect of silica and isolation approach, Colloids Surf, A 552 (2018) 130–141, https://doi.org/ 10.1016/j.colsurfa.2018.04.070.
- [45] W.H. Simpson, G.H. Crawshaw, Wool: Science and Technology, Woodhead Publishing Limited, Cambridge, 2002.
- [46] M. Montazer, E. Pakdel, Reducing photoyellowing of wool using nano TiO₂, Photochem, Photobiol 86 (2010) 255–260, https://doi.org/10.1111/j.1751-1097 2009 00680 x
- [47] M. Montazer, E. Pakdel, M.B. Moghadam, The role of nano colloid of TiO₂ and butane tetra carboxylic acid on the alkali solubility and hydrophilicity of proteinous fibers, Colloids Surf, A 375 (2011) 1–11, https://doi.org/10.1016/j. colsurfa 2010 10 051
- [48] H. Barani, A. Haji, Chapter 13 spectroscopic studies on wool fibers, in: S. Jose, S. Thomas, G. Basu (Eds.), The Wool Handbook, Woodhead Publishing, 2024, pp. 309–326, https://doi.org/10.1016/B978-0-323-99598-6.00025-6.
- [49] A. Shavandi, M.A. Ali, Graft polymerization onto wool fibre for improved functionality, Prog, Org, Coat 130 (2019) 182–199, https://doi.org/10.1016/j. porgcoat.2019.01.054.
- [50] D.N.G. Krishna, J. Philip, Review on surface-characterization applications of X-ray photoelectron spectroscopy (XPS): recent developments and challenges, Appl, Surf, Sci, Adv 12 (2022) 100332, https://doi.org/10.1016/j.apsadv.2022.100332.
- [51] R. Molina, J.P. Espinós, F. Yubero, P. Erra, A.R. González-Elipe, XPS analysis of down stream plasma treated wool: influence of the nature of the gas on the surface modification of wool, Appl, Surf, Sci 252 (2005) 1417–1429, https://doi.org/ 10.1016/j.apsusc.2005.02.147.
- [52] L. Wang, Z. Duan, P. Fei, Z. Yan, W. Wang, Y. Di, J. Lu, An eco-friendly rapid shrink-proofing finishing of wool fibers by protease based on substrate activation strategy, Colloids Surf, A: Physicochem, Eng, Asp 709 (2025) 136215, https://doi. org/10.1016/j.colsurfa.2025.136215.
- [53] Y. Zhang, N. Zhang, Q. Wang, Y. Yu, P. Wang, J. Yuan, A facile and controllable approach for surface modification of wool by micro-dissolution, Fibers Polym 21 (2020) 1229–1237, https://doi.org/10.1007/s12221-020-9727-9.
- [54] H. Zhang, H. Yan, N. Mao, Functional modification with TiO₂ nanoparticles and simultaneously dyeing of wool fibers in a one-pot hydrothermal process, Ind, Eng, Chem, Res 53 (2014) 2030–2041, https://doi.org/10.1021/ie402966z.
- [55] Z. Jiang, N. Zhang, Q. Wang, P. Wang, Y. Yu, J. Yuan, A controlled, highly effective and sustainable approach to the surface performance improvement of wool fibers, J. Mol, Liq 322 (2021) 114952, https://doi.org/10.1016/j.molliq.2020.114952.
- [56] S. Enkhzaya, K. Shiomori, B. Oyuntsetseg, Effective adsorption of Au(III) and Cu(II) by chemically treated sheep wool and the binding mechanism, J. Env., Chem, Eng 8 (2020) 104021, https://doi.org/10.1016/j.jece.2020.104021.
- [57] P. Rajaram, A.R. Jeice, K. Jayakumar, Review of green synthesized TiO2 nanoparticles for diverse applications, Surf, Interfaces 39 (2023) 102912, https://doi.org/10.1016/i.surfin.2023.102912.
- [58] V.H. Rathi, A.R. Jeice, K. Jayakumar, Green synthesis of Ag/CuO and Ag/TiO₂ nanoparticles for enhanced photocatalytic dye degradation, antibacterial, and antifungal properties, Appl, Surf, Sci, Adv 18 (2023) 100476, https://doi.org/10.1016/j.apsadv.2023.100476.
- [59] M. Simonič, V. Flucher, T. Luxbacher, A. Vesel, L.Fras Zemljič, Adsorptive removal of heavy metal ions by waste wool, J. Nat. Fibers 19 (2022) 14490–14503, https:// doi.org/10.1080/15440478.2022.2064401.
- [60] N. Kohara, M. Kanei, T. Nakajima, Effect of reduction and succinylation on water absorbance of wool fibers, Tex. Res. J 71 (2001) 1095–1098, https://doi.org/ 10.1177/004051750107101210.
- [61] N. Kohara, T. Nakajima, Influence of succinylation on the interactions of wool fibers and water, Tex. Res. J 74 (2004) 856–860, https://doi.org/10.1177/ 004051750407401003.
- [62] H. Zhang, K.R. Millington, X. Wang, The photostability of wool doped with photocatalytic titanium dioxide nanoparticles, Polym, Degrad, Stab 94 (2009) 278–283, https://doi.org/10.1016/j.polymdegradstab.2008.10.009.
- [63] K.R. Millington, C. Deledicque, M.J. Jones, G. Maurdev, Photo-induced chemiluminescence from fibrous polymers and proteins, Polym, Degrad, Stab 93 (2008) 640–647, https://doi.org/10.1016/j.polymdegradstab.2008.01.006.
- [64] H. Zhang, S. Deb-Choudhury, J. Plowman, K. Millington, J. Dyer, The influence of copper(II) ions on wool photostability in the dry state, Color, Technol 129 (2013) 323–329, https://doi.org/10.1111/cote.12039.
- [65] K.R. Millington, H. Zhang, M.J. Jones, X. Wang, The effect of dyes on photoinduced chemiluminescence emission from polymers, Polym, Degrad, Stab 95 (2010) 34–42, https://doi.org/10.1016/j.polymdegradstab.2009.10.014.
- [66] E. Pakdel, W.A. Daoud, L. Sun, X. Wang, Photostability of wool fabrics coated with pure and modified TiO₂ colloids, J. Colloid Interface Sci 440 (2015) 299–309, https://doi.org/10.1016/j.jcis.2014.10.032.
- [67] R. Qian, H. Zong, J. Schneider, G. Zhou, T. Zhao, Y. Li, J. Yang, D.W. Bahnemann, J.H. Pan, Charge carrier trapping, recombination and transfer during ${\rm TiO_2}$

- photocatalysis: an overview, Catal. Today 335 (2019) 78–90, https://doi.org/ 10.1016/j.cattod.2018.10.053.
- [68] C. Canal, P. Erra, R. Molina, E. Bertrán, Regulation of surface hydrophilicity of plasma treated wool fabrics, Tex, Res, J 77 (2007) 559–564, https://doi.org/ 10.1177/0040517507078062.
- [69] D. Chen, L. Tan, H. Liu, J. Hu, Y. Li, F. Tang, Fabricating superhydrophilic wool fabrics, Langmuir 26 (2009) 4675–4679, https://doi.org/10.1021/la903562h.
- [70] E. Pakdel, W.A. Daoud, X. Wang, Self-cleaning and superhydrophilic wool by TiO₂/SiO₂ nanocomposite, Appl, Surf, Sci 275 (2013) 397–402, https://doi.org/10.1016/j.apsusc.2012.10.141.
- [71] W. Xie, E. Pakdel, Y. Liang, D. Liu, L. Sun, X. Wang, Natural melanin/TiO₂ hybrids for simultaneous removal of dyes and heavy metal ions under visible light, J. Photochem, Photobiol, A 389 (2020) 112292, https://doi.org/10.1016/j. jphotochem.2019.112292.
- [72] W. Xie, E. Pakdel, D. Liu, L. Sun, X. Wang, Waste-hair-derived natural melanin/ TiO₂ hybrids as highly efficient and stable UV-shielding fillers for polyurethane films, ACS Sustain. Chem, Eng (2019), https://doi.org/10.1021/ acssuschemeng.9b03514.
- [73] E. Pakdel, W.A. Daoud, R.J. Varley, X. Wang, Antibacterial textile and the effect of incident light wavelength on its photocatalytic self-cleaning activity, Mater, Lett 318 (2022) 132223, https://doi.org/10.1016/j.matlet.2022.132223.

- [74] M.A. Vargas, J.E. Rodríguez-Páez, Facile synthesis of TiO₂ nanoparticles of different crystalline phases and evaluation of their antibacterial effect under dark conditions against E. coli, J Clust Sci 30 (2019) 379–391, https://doi.org/10.1007/ s10876-019-01500-3.
- [75] N.K. Gali, Z. Ning, W. Daoud, P. Brimblecombe, Investigation on the mechanism of non-photocatalytically TiO2-induced reactive oxygen species and its significance on cell cycle and morphology, J. Appl, Toxicol 36 (2016) 1355–1363, https://doi. org/10.1002/jat.3341.
- [76] C.C. Mercado, F.J. Knorr, J.L. McHale, S.M. Usmani, A.S. Ichimura, L.V. Saraf, Location of hole and electron traps on nanocrystalline anatase TiO₂, J. Phys. Chem. C 116 (2012) 10796–10804, https://doi.org/10.1021/jp301680d.
- [77] M. Ajdary, M.A. Moosavi, M. Rahmati, M. Falahati, M. Mahboubi, A. Mandegary, S. Jangjoo, R. Mohammadinejad, R.S. Varma, Health concerns of various nanoparticles: a review of their in vitro and in vivo toxicity, Nanomaterials 8 (2018) 634, https://doi.org/10.3390/nano8090634.
- [78] Q. Guo, D. Wei, C. Zhao, C. Wang, H. Ma, Y. Du, Physical UV-blocker TiO₂ nanocomposites elevated toxicity of chemical sunscreen BP-1 under UV irradiation, Chem, Eng, J 469 (2023) 143899, https://doi.org/10.1016/j.cej.2023.143899.
- [79] P. Ganguly, A. Breen, S.C. Pillai, Toxicity of nanomaterials: exposure, pathways, assessment, and recent advances, ACS Biomater, Sci, Eng 4 (2018) 2237–2275, https://doi.org/10.1021/acsbiomaterials.8b00068.